MOSSBAUER EFFECT REFERENCE AND DATA JOURNAL, 3 (1980) 154-163
Mossbauer Effect Data Center, Asheville NC 28814, USA

GEOMETRIC EFFECTS IN MÖSSBAUER TRANSMISSION EXPERIMENTS

J. J. Bara and B. F. Bogacz

Institute of Physics, Jagiellonian University
Reymonta 4, 30-059 Cracow, Poland

The influence of geometric effects on the shape, the width, the position and the amplitude of a Mössbauer absorption line is numerically analyzed and experimentally studied. The geometric effects decrease the energy resolution of Mössbauer spectroscopy, induce non-linearity in the velocity scale and reduce the amplitude of a Mössbauer line.

I. INTRODUCTION

Mössbauer spectroscopy has become a powerful tool in various fields of investigation. Its most frequently utilized properties are the high energy resolution, the short observation time and the large value of the nuclear resonance cross section. They have a great influence on the shape of the Mössbauer spectrum which is determined mainly by the hyperfine interactions of the nuclei with their electronic shells. However, a Mössbauer spectrum is usually more or less deformed due to several reasons. One of them, the geometric arrangement in a Mössbauer transmission experiment, is analyzed in this paper. The so-called cosine smearing of the energy distribution of recoillessly emitted gamma rays and the periodical changes of the source-detector solid angle are the most serious geometric effects.

II. COSINE SMEARING OF THE ENERGY DISTRIBUTION

When the direction of a photon emitted by a point source forms an angle θ with the direction of the source velocity, the Doppler energy shift is given by $\Delta E = V\cos\theta$, where $V = vE_o/c$, E_o is the mean value of the photon energy, while v and c are source and light velocities, respectively. This $\cos\theta$ term changes the energy distribution of the gamma ray beam recoillessly emitted within the solid angle $2\pi(1-\cos\alpha)$ about the direction of the source velocity. The new energy distribution is no longer of a Lorentzian type and is given by formula (1)

$$U(E,V,\alpha) = \int_0^{2\pi} d\varphi \int_0^{\alpha} \sin\theta\, U(E,V,\theta)\, d\theta, \qquad (1)$$

where

$$U(E,V,\theta) = \frac{2}{\pi\Gamma}\, \frac{(\Gamma/2)^2}{[E-(E_o+V\cos\theta)]^2+(\Gamma/2)^2}\,. \qquad (2)$$

E and E_o are the energies of an emitted photon and the Mössbauer energy level, while Γ is the width of the energy distribution for $\theta = 0$. Integrating Eq. (1) over the angles φ and θ we have

$$U(E,V,\alpha) = \frac{2}{V}\,\mathrm{arctg}\,\frac{2}{\Gamma}[E-(E_o+V\cos\alpha)] - \mathrm{arctg}\,\frac{2}{\Gamma}[E-(E_o+V)]\,. \qquad (3)$$

The cosine effect symmetrically broadens the energy distribution and shifts its maximum from $E_o + V$ towards E_o. This is shown in Figs. 1 and 2, where two sets of the energy distributions calculated from Eq. (3) for various angles α and various Doppler energy shifts V are shown, respectively. The energy distribution described by Eq. (3) reaches its maximum value

$$U(E_m, V,\alpha) = \frac{4}{V}\,\mathrm{arctg}\,\frac{V(1-\cos\alpha)}{\Gamma} \qquad (4)$$

at the energy

$$E_m = E_o + V\frac{1+\cos\alpha}{2}\quad . \qquad (5)$$

It is shifted on the energy scale from $E_o + V$ towards E_o by the value

$$\Delta E = \frac{V(1-\cos\alpha)}{2}\quad . \qquad (6)$$

The width of the energy distribution at its half maximum is given by the formula

$$\Gamma_\alpha = \sqrt{V^2(1-\cos\alpha)^2+\Gamma^2}\quad . \qquad (7)$$

Its dependences of the angle α and the Doppler energy shift V are illustrated in Figs. 3 and 4, respectively.

The cosine smearing of the energy distribution has a great influence on the Mössbauer spectrum.

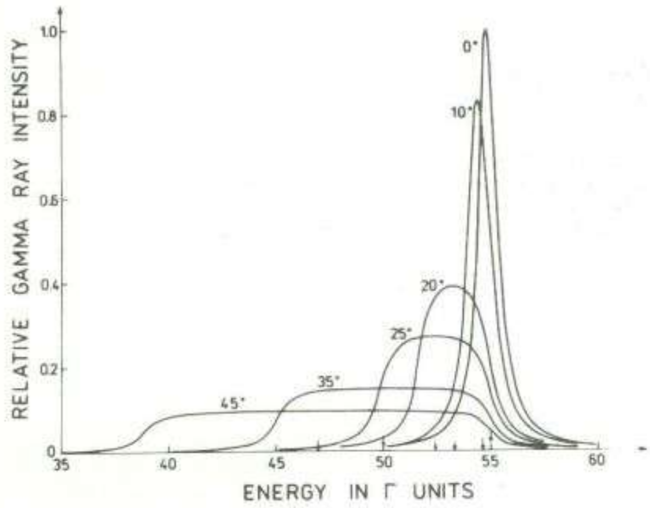

FIG. 1. Energy distributions calculated from Eq. (3) for the Doppler energy shift $V = 55\Gamma$ and various angles α. The arrows indicate positions of the distribution maxima on the energy scale. The energy of gamma rays is given with respect to E_o and is expressed in Γ units. All distributions are normalized to the same area.

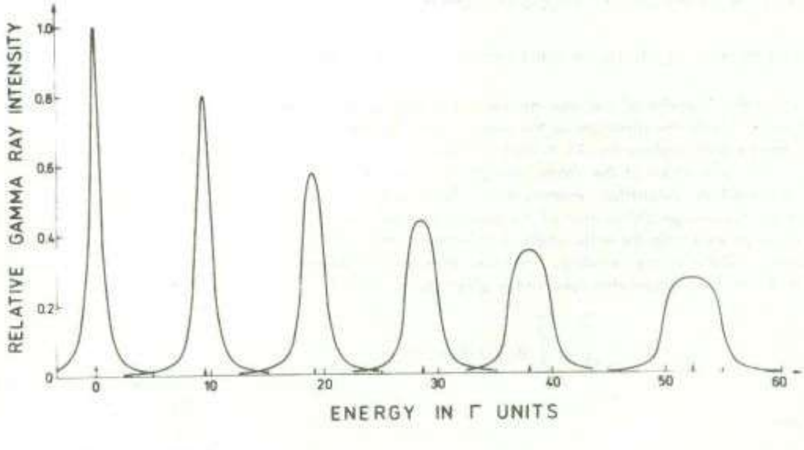

FIG. 2. Energy distributions calculated from Eq. (3) for $\alpha = 25°$ and Doppler energy shifts $V = 0$, 10, 20, 30, 40 and 55Γ. The arrows indicate the positions of the distribution maxima on the energy scale. Energy of gamma rays is given with respect to E_o and is expressed in Γ units. All distributions are normalized to the same area.

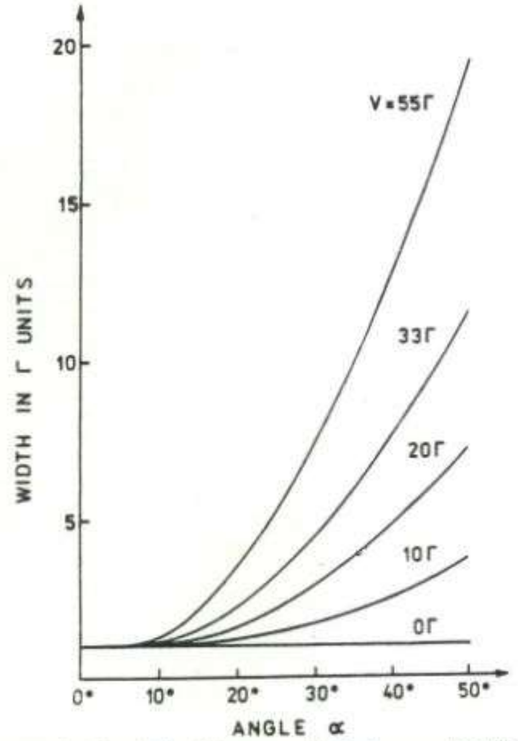

FIG. 3. The widths of the energy distributions as a function of the angle α calculated from Eq. (3) for various Doppler energy shifts V.

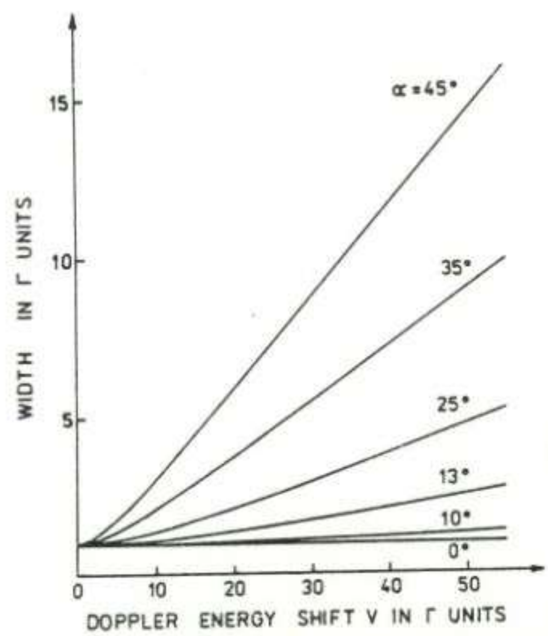

FIG. 4. The widths of the energy distributions as functions of the Doppler energy shift V calculated from Eq. (3) for various angles α.

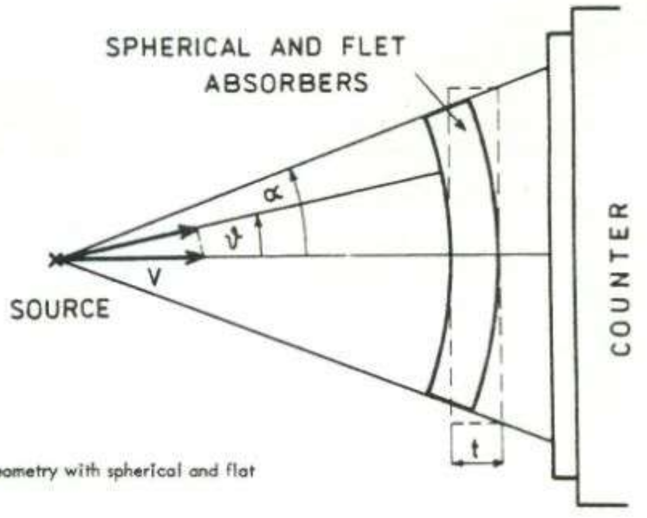

FIG. 5. Transmission geometry with spherical and flat Mössbauer absorbers.

III. COSINE SMEARING OF A MÖSSBAUER ABSORPTION LINE

A flat absorber is thicker for gamma rays emitted at a given angle than for those emitted at $\theta = 0$. Thus, in calculating the shape of a Mössbauer line both the cosine smearing of the energy distribution and θ-dependent thickness effect have to be taken into account. In order to study the influence of a pure cosine smearing of energy distribution on a Mössbauer absorption line, one has to consider the spherical geometry shown in Fig. 5. The point Mössbauer source, located in the geometrical center of the sphere, is moved with a constant acceleration. The gamma rays emitted radially within the solid angle $2\pi(1-\cos\alpha)$ interact with the spherical absorber of thickness t. The amplitude of the source vibration is supposed to be very small in comparison to the radius of the sphere. The intensity of gamma rays which have passed the absorber is registered in the memory of the multichannel analyzer as a function of the source velocity.

The background corrected Mössbauer line

$$\mathcal{E}(V) = [N(\infty) - N(V)]/N(\infty) \tag{8}$$

measured for a spherical absorber is described by formula

$$\mathcal{E}(V) = f_o \int_0^\infty \frac{U(E, V, \alpha)}{2\pi(1-\cos\alpha)} \left\{1 - \exp\left[-\mu_r(E, E_r)\,t\right]\right\} dE \tag{9}$$

$N(V)$ and $N(\infty)$ are the numbers of counts at a given Doppler energy shift V and at $V = \infty$, respectively. f_o is the source Debye-Waller factor, while $\mu_r(E, E_r)$ is the nuclear resonance absorption coefficient for the absorber used in the experiment. The resonance energy of the absorber is denoted by E_r.

For a flat absorber the shape of the background corrected absorption line is described by formula

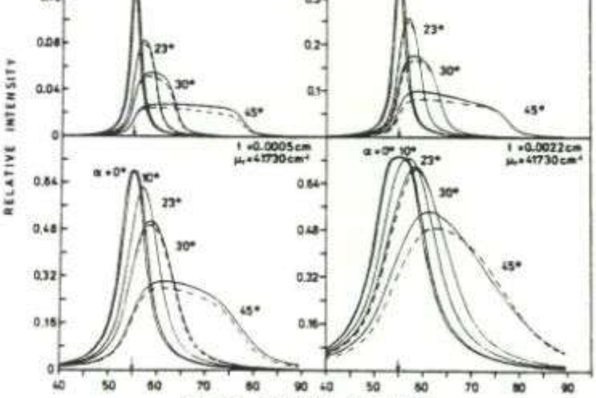

FIG. 6. Mössbauer absorption lines calculated for flat (solid lines) and spherical (dashed lines) absorbers of various thicknesses t and various nuclear resonance coefficients μ_r. Calculations were performed for various angles α. Arrows indicate resonance velocities for $\alpha = 0°$.

$$\mathcal{E}(V) = \frac{f_o \int_0^\infty dE \int_0^\alpha d\theta \sin\theta\, U(E, V, \theta) \exp(-\mu\, t\sec\theta) \left\{1 - \exp\left[-\mu_r(E_r)\, t\sec\theta\right]\right\}}{\int_0^\alpha d\theta \sin\theta \exp(-\mu\, t\sec\theta)} \,. \tag{10}$$

Formula (10) can be transformed to its simplified form (9) by substituting t for $t\sec\alpha$, which is the actual case, not an approximation for a spherical absorber.

Eqs. (9) and (10) were used in numerical calculations of the shape of the Mössbauer lines for various angles, nuclear resonance absorption coefficients μ_r, and absorber thicknesses t. The cosine effect broadens the Mössbauer line, shifts it towards higher velocities and diminishes the magnitude of the Mössbauer effect. This is shown in Fig. 6 for flat and spherical absorbers. The decrease in the intensity of gamma rays transmitted through the flat absorber at large θ angles diminishes the influence of the outermost part of the absorber on the shape of a Mössbauer line. This can be clearly noticed for large angles α. The width of a Mössbauer line, its position and the magnitude of the Mössbauer effect are sensitive functions of the angle α and the resonance energy.

These dependences (Figs. 7-14) were calculated from Eqs. (9) and (10) for a $2.2 \cdot 10^{-3}$ cm thick non-enriched absorber like a hypothethical metallic iron foil with zero hyperfine splittings at room temperature. The resonance energy of the hypothethical absorber is given with respect to the source and and is expressed in Γ units. It was located at various positions on the energy scale in studying the influence of a Doppler energy shift on line parameters. The broadening of the Mössbauer line due to the $\cos\theta$ effect (Figs. 7 and 8) decreases the energy resolution of Mössbauer spectroscopy. The shift of the Mössbauer line (Figs. 9 and 10) towards higher velocities induces nonlinearity (Fig. 11) in the velocity scale of Mössbauer spectra. The decrease in magnitude of the Mössbauer effect (Figs. 12-14) is associated with line broadening. For large angles α the magnitude of the Mössbauer effect saturates more slowly (Fig. 14) with an increase in absorber thickness than for $\alpha = 0$.

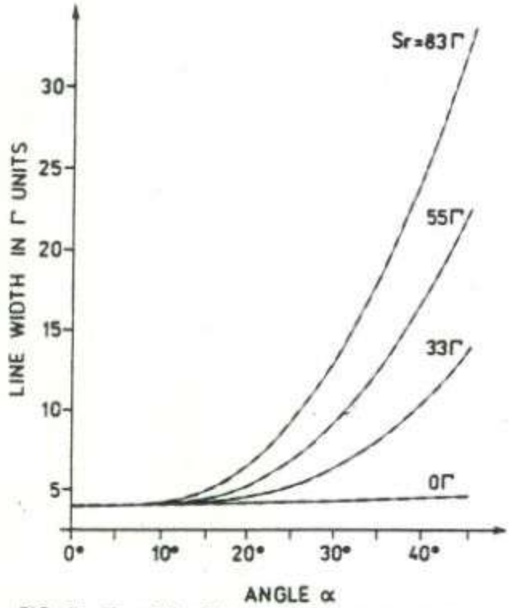

FIG. 7. The widths of Mössbauer lines for flat (solid lines) and spherical (dashed lines) absorbers as functions of the angle α calculated for various resonance energies (S_r). S_r is given with respect to the source and is expressed in Γ units.

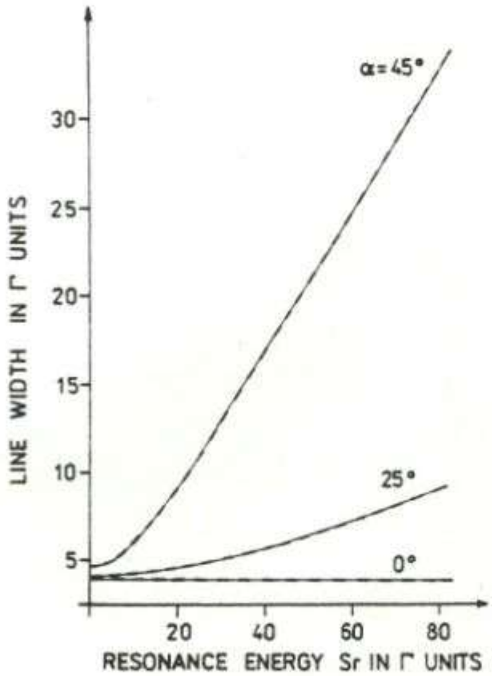

FIG. 8. The widths of Mössbauer lines for flat (solid lines) and spherical (dashed lines) absorbers as functions of resonance energy (S_r) calculated for various angles α. S_r is given with respect to the source and is expressed in Γ units.

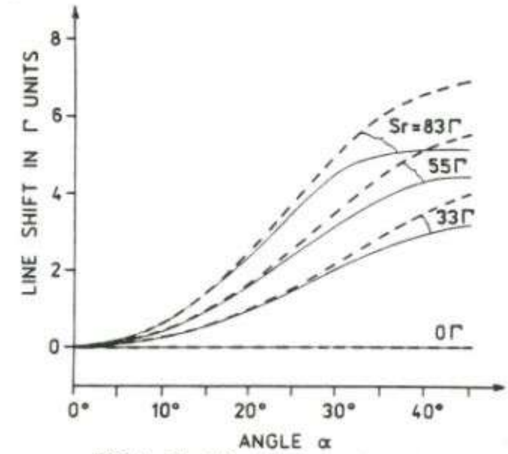

FIG. 9. The shifts of the line position for flat (solid lines) and spherical (dashed lines) absorbers as functions of the angle α calculated for various resonance energies (S_r). S_r is given with respect to the source and is expressed in Γ units.

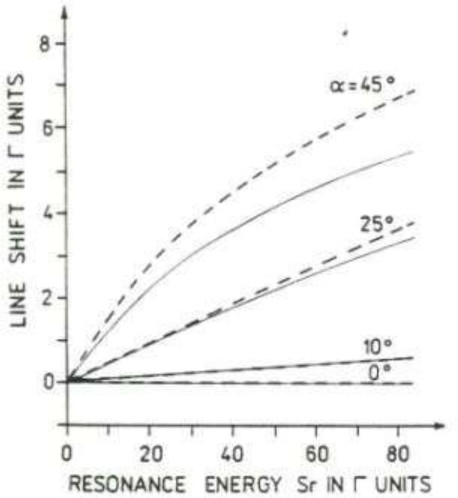

FIG. 10. The shifts of the line position for flat (solid lines) and spherical (dashed lines) absorbers as functions of resonance energy (S_r) calculated for various angles α. S_r is given with respect to the source and is expressed in Γ units.

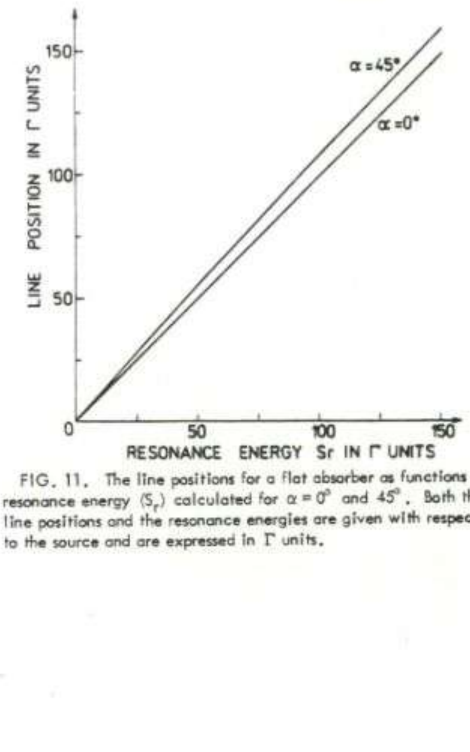

FIG. 11. The line positions for a flat absorber as functions of resonance energy (S_r) calculated for $\alpha = 0^\circ$ and 45°. Both the line positions and the resonance energies are given with respect to the source and are expressed in Γ units.

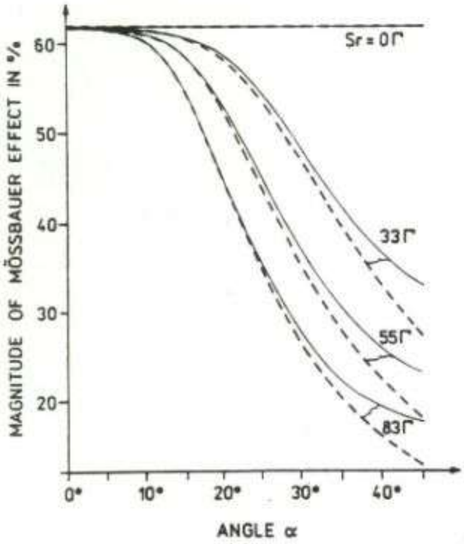

FIG. 12. The magnitudes of the Mössbauer effect for flat (solid lines) and spherical (dashed lines) absorbers as functions of the angle α calculated for various resonance energies (S_r). S_r is given in respect to the source and is expressed in Γ units.

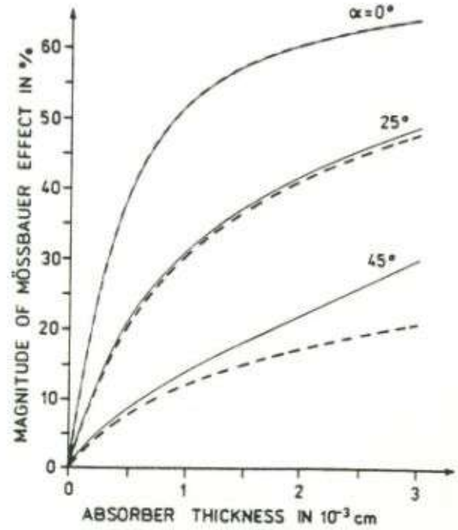

FIG. 14. The magnitudes of the Mössbauer effect for flat (solid lines) and spherical (dashed lines) absorbers as functions of absorber thickness calculated for resonance energy $S_r = 55\,\Gamma$ and various angles α. S_r is given with respect to the source.

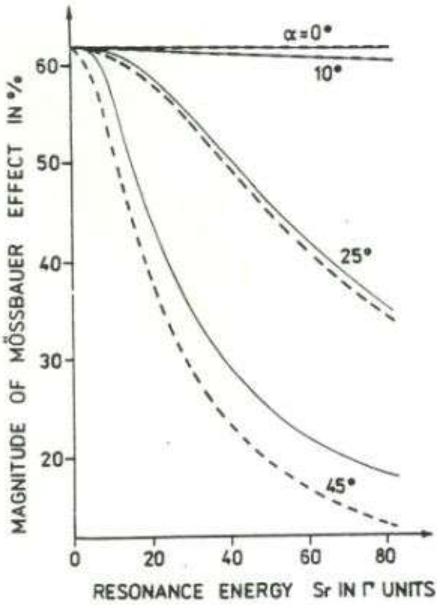

FIG. 13. The magnitudes of the Mössbauer effect for flat (solid lines) and spherical (dashed lines) absorbers as functions of resonance energy (S_r) calculated for various angles. S_r is given with respect to the source and is expressed in Γ units.

The influence of the $\cos\theta$ effect on the shape of the Mössbauer Zeeman spectrum was studied experimentally for $2.2\cdot10^{-3}$cm thick non-enriched metallic iron foil. Figs. 15 and 16 show absorption Zeeman spectra measured for $\alpha = 5^\circ$, 10°, 23.3° and for $\alpha = 31.3^\circ$, 38°, respectively. The dashed lines represent the Zeeman spectra calculated for $\alpha = 0^\circ$. The solid lines represent the spectra with the $\cos\theta$ effect included which were calculated for a flat absorber. The influence of the $\cos\theta$ effect on Zeeman spectra is clearly seen for $\alpha > 10^\circ$. For the angles $\alpha < 10^\circ$ the shape of the Zeeman spectra is well described both by Eq. (9) and Eq. (10). Eq. (10) gives better results for large angles α as is indicated in Fig. 16 (thick solid line). In order to get satisfactory agreement for large angles α between the solid line and the experimental points one has to include in the calculations the source dimensions and θ-dependent self absorption in the source. This was not done in our calculations.

IV. PARABOLIC LIKE GEOMETRIC EFFECT

The source vibrations induce the periodic changes of the source-detector solid angle and cause the count rate to be, in the first approximation, a parabolic like function of the source velocity. The magnitude of this geometric effect observed without the Mössbauer absorber, $G = [N(\infty) - N(0)]/N(\infty)$, strongly decreases with the decrease in the ratio of the source vibration amplitude to the source-detector separation. These magnitudes G have opposite signs and slightly different values for two spectra (left and right) taken within one period of the velocity sweep (Fig. 17). The influence of the parabolic like geometric effect on the Mössbauer spectra can not be ignored for geometries commonly used in Mössbauer effect experiments. It can be greatly reduced (Fig. 17) by folding two Mössbauer spectra (left and right) with respect to their mirror image. Very often a simple parabolic correction is included in a fitting procedure. In precise Mössbauer effect measurements the source dimensions and both $\cos\theta$ and parabolic like geometric effects should be taken into account. However, it is not easy to do so, especially for complex Mössbauer spectra. The parabolic like geometric effect is most distinctly pronounced for large source vibration amplitudes and for very small magnitudes of the Mössbauer effect. Fig. 18 shows Zeeman spectra measured for a very thin ($5\cdot10^{-5}$cm) non-enriched metallic iron foil. The solid lines represent the theoretical curves in which both $\cos\theta$ and parabolic like geometric effects are included.

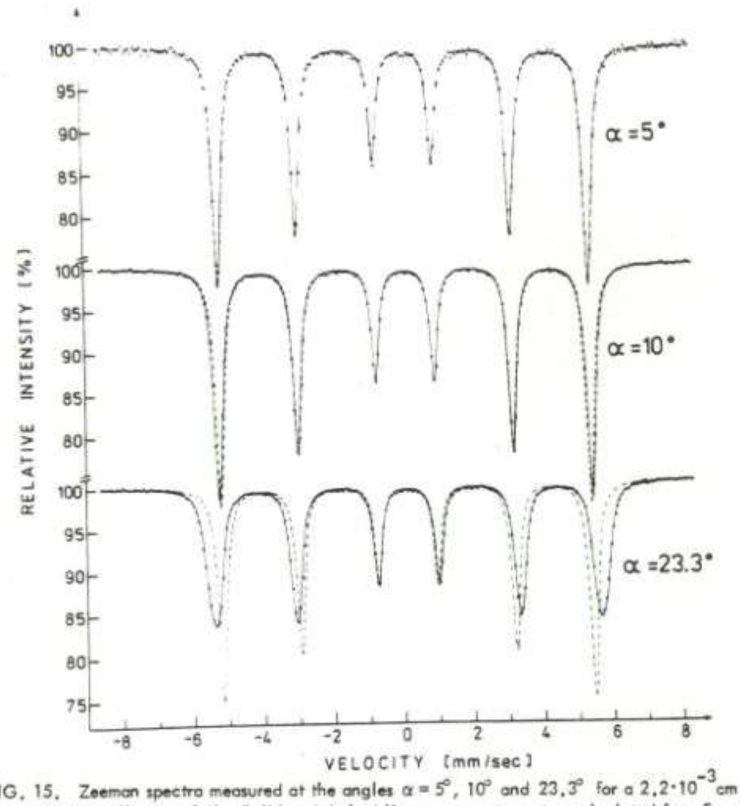

FIG. 15. Zeeman spectra measured at the angles $\alpha = 5^\circ$, 10° and 23.3° for a $2.2\cdot10^{-3}$cm thick non-enriched metallic iron foil. Solid and dashed lines represent spectra calculated from Eq. (11) for the angles α used in the experiment and for $\alpha = 0^\circ$, respectively.

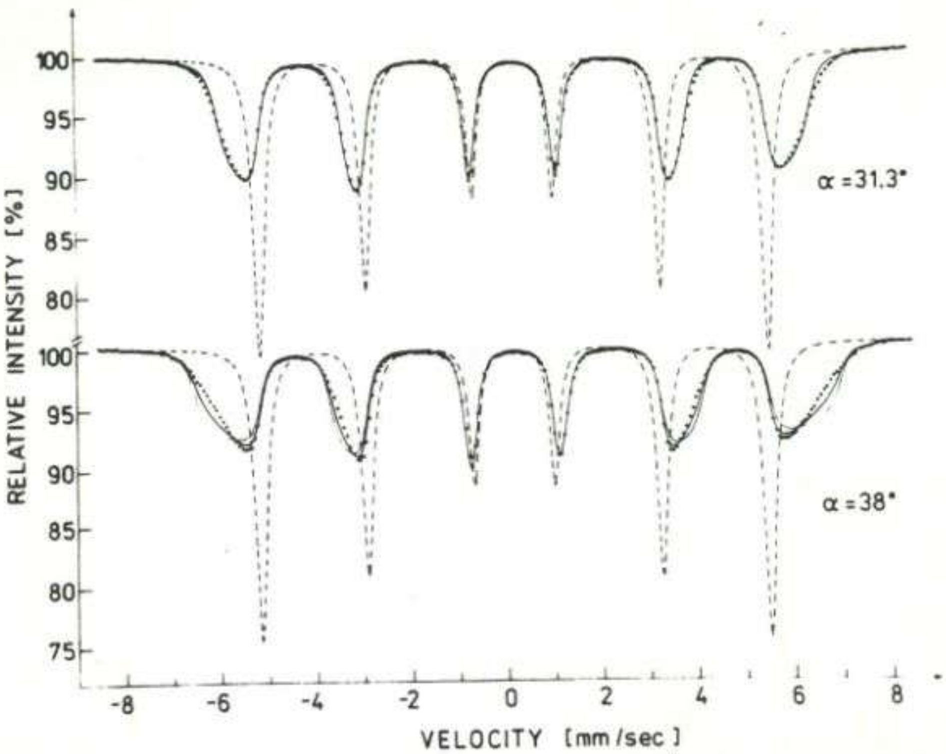

FIG. 16. Zeeman spectra measured at angles $\alpha = 31.3^\circ$ and 38° for a $2.2 \cdot 10^{-3}$ cm thick non-enriched metallic iron foil. Thick solid and dashed lines represent spectra of flat absorbers calculated for angles α used in the experiments and for $\alpha = 0^\circ$, respectively. Thin solid line was calculated for spherical absorber.

FIG. 17. The magnitude of the parabolic like geometric effect as a function of the ratio of the source vibration amplitude X to the source-detector separation R. Various ratios of the detector diameter h to the source-detector separation R were considered in the calculations.

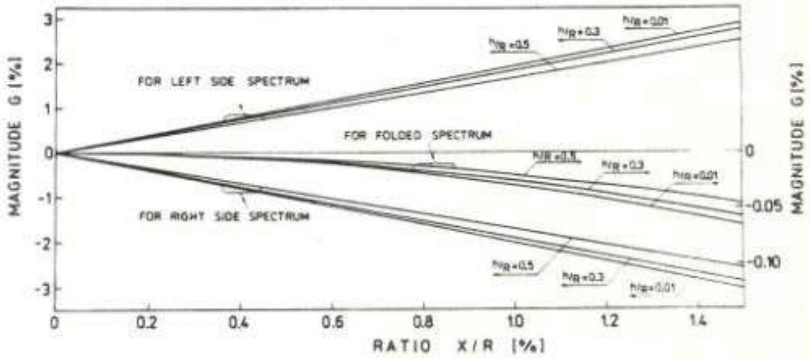

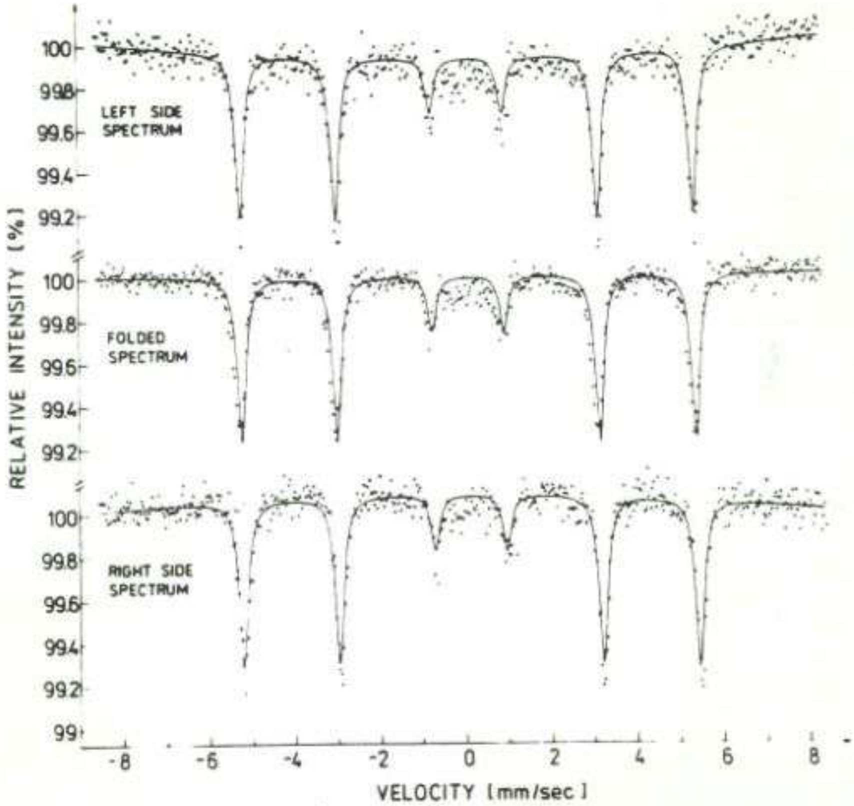

FIG. 18. Zeeman spectra measured for $5\cdot10^{-5}$cm thick non-enriched metallic iron foil. Solid lines represent theoretical spectra with the $\cos\theta$ and parabolic like geometric effects included.

REFERENCES

[1] J. J. Spijkerman, F. C. Ruegg, and J. R. DeVoe, in Mössbauer Effect Methodology, Volume 1 (Plenum, New York, 1965), p. 119.

[2] C. Nistror and T. Tinu, Rev. Roum. Phys. 11, 551 (1966).

[3] R. Riesenman, J. Steger, and L. Kostinev, Nucl. Instrum. Methods 72, 109 (1969).

[4] P. Gütlich, R. Link, and A. Trautwein, Mössbauer Spectroscopy and Transition Metal Chemistry (Springer-Verlag, Berlin, 1978).